Direct Measurement of High Frequency, Solid Propellant, Pressure-Coupled Admittances

J. R. Wilson* and M. M. Micci†
The Pennsylvania State University, University Park, Pennsylvania

This paper presents an experimental method that is capable of directly measuring solid propellant pressure-coupled responses at the high frequencies associated with tangential mode instabilities inside solid propellant rocket motors. The method utilizes a magnetic flowmeter to measure the velocity oscillation above a burning propellant surface simultaneously with a pressure oscillation measurement within an externally excited combustion chamber. A magnetic flowmeter burner was designed and constructed to evaluate this method of pressure-coupled response measurement. Response measurements were obtained for two formulations of AP/HTPB composite propellant at pressure oscillation frequencies of 4000 and 8000 Hz. The measurement data displayed repeatable trends in both the real and imaginary parts of the pressure-coupled response function.

Nomenclature

a = speed of sound
A_b = admittance function
B = manetic flux density
L = electrode separation distance
m = mass flow
M_b = Mach number of gas leaving burning propellant surface
P = pressure
R_b = response function
U = flow velocity
U_b = velocity of gas leaving burning propellant surface
V = voltage
α = flowmeter constant
γ = ratio of specific heats

Superscripts

$(\bar{\ })$ = mean quantity
$(')$ = fluctuating quantity

Introduction

THE experimental measurement of solid propellant response functions, both pressure- and velocity-coupled, are critical input parameters for rocket motor stability analyses. There have been several experimental techniques developed to measure propellant pressure-coupled response functions,[1,2] such as the T-burner, rotating value burner, impedance tube, tangential mode burner, and microwave burner. All of these techniques, with the exception of the microwave burner, involve an indirect measurement of the propellant response function. The indirect measurement deduces a propellant response by utilizing an analytical model of the unsteady gasdynamics and combustion process occurring in the burner to reproduce the measured pressure oscillations. This method requires a complete understanding of all the physical processes, both gasdynamic and combustion related, occurring in the particular experimental device in order to relate the propellant response to the pressure measurements. The analysis forces the propellant response to be only as accurate as the assumed physical processes occurring in the combustion chamber. Only two devices, the tangential mode burner and the slot vent T-burner, are able to make response measurements at frequencies greater than 1000 Hz. The problem of high-frequency combustion instability in solid propellant rocket motors has previously been averted by the use of metallic powders, which provide excellent high frequency damping. However, in the move back toward smokeless propellants, it has become necessary to remove the metal particulates and the problem of propellant response at high frequencies has reappeared.

A magnetic flowmeter is theoretically capable of obtaining a direct measurement of the gas velocity above a burning solid propellant surface with a frequency response greater than 20 kHz. The operation of a magnetic flowmeter is based on the principle first discovered by Faraday that a conducting gas (or any medium) moving through a magnetic field will generate an electrical potential that is normal to both the magnetic field and the flow velocity. The potential, which can be measured as a voltage, is proportional to the magnitude of the flow velocity and to the magnetic field strength. The measurement of the oscillatory gas velocity above a burning solid propellant surface subjected to pressure oscillations constitutes a direct measurement of the propellant pressure-coupled admittance and is the basis of the experimental portion of this program.

The admittance is defined as the nondimensional ratio of the combustion gas velocity to the oscillatory pressure,

$$A_b = \frac{U_b'/\bar{a}}{P'/\gamma\bar{P}} \tag{1}$$

where primes denote fluctuating quantities and overbars a mean quantity. The oscillatory velocity U_b' is nondimensionalized by the mean sonic velocity within the combustion chamber, $\bar{a}$. The pressure-coupled response is the nondimensional ratio of the mass flow oscillation to the oscillatory pressure:

$$R_b = \frac{m'/\bar{m}}{P'/\bar{P}} \tag{2}$$

Presented as Paper 85-113 at the AIAA/SAE/ASME/ASEE 21st Joint Propulsion Conference, Monterey, CA, June 8-10,1985; received Feb. 11, 1986; revision submitted July 31, 1986.

*Graduate Research Assistant, Department of Aerospace Engineering. Currently Member of Technical Staff, General Electric Company, Springfield, VA. Member AIAA.

†Assistant Professor, Department of Aerospace Engineering. Member AIAA.

The response and admittance functions are related for isentropic fluctuations by the equation

$$A_b + \bar{M}_b = \gamma \bar{M}_b R_b \tag{3}$$

where $\bar{M}_b$ is the mean Mach number of the product gases as they leave the propellant surface. A magnetic flowmeter is capable of directly measuring the oscillatory velocity U_b' which, in conjunction with the oscillatory pressure P' (simultaneously measured by a pressure transducer), produces the direct measurement of the propellant admittance.

The magnetic flowmeter operates according to Faraday's law, which states that a conductor moving relative to a magnetic field will generate an electrical potential proportional to the flow velocity.[3] The potential in volts V is given by

$$V = \alpha UBL \tag{4}$$

where α is a nondimensional calibrating constant of order unity, U the flow velocity (m/s), B the magnetic flux density (T) and L the distance across which the potential is being measured. This phenomenon is shown schematically in Fig. 1. Although Eq. (4) shows that the potential is independent of gas or fluid conductivity, electrical conductivity limits exist for which the equation holds true. In the upper limit, a highly ionized flow could allow magnetohydrodynamic forces to distort the velocity profile. The lower limit for conductivity is approximately 10^{-3} mhos/m, below which the electrical resistance of the gas between the voltage measuring electrodes grows to become of the same order of magnitude as the input impedance of the voltage measuring instrumentation, resulting in current flow between the electrodes and subsequent measurement errors. Micci and Caveny[4,5] demonstrated that the electrical conductivity is within these limits for a composite propellant when they measured the mean and unsteady velocities within a solid propellant combustion chamber. Sufficient electrical conductivity is obtained for a composite propellant due to trace amounts of sodium and potassium contained in the ammonium perchlorate.

Experimental Apparatus

The magnetic flowmeter assembly is schematically depicted in Fig. 2. This figure presents the major components necessary for surface admittance measurement. Pressure oscillations are produced by the pressure modulation system (A), which is located at the converging nozzle orifice. The pressure oscillations are measured simultaneously with the oscillatory velocity as the propellant strand burns by the measurement station shown in the cutaway section (B). The large external magnet (C) provides a large dc magnetic field for the velocity measurement obtained by measuring the voltage across the electrodes at the measurement station. The combustion chamber (D) was designed to require small amounts of propellant (4.0 cm^3) for each run. A cutaway side view of the magnetic flowmeter burner is shown in Fig. 3. The interior dimensions of the combustion chamber were 1.27 cm in diameter and 6.75 cm in length, with the velocity electrodes and the oscillatory pressure transducer located at the same axial position. The propellant samples were formed into cylindrical strands with a diameter of 1.2 cm and a length of 3.5 cm. The small propellant requirement makes the burner very economical to run and, hence, allows a wide variety of propellants to be investigated. The electrodes were 2% thoriated tungsten rods with a diameter of 1.6 mm. The electrodes penetrated 3.0 mm into the propellant strand resulting in a separation distance of 6.0 mm. The electrodes measure a velocity integrated over a line between the two electrodes. For axisymmetric flows, like those occurring in the magnetic flowmeter burner, the integration yields the mass-averaged mean flow in the plane containing the two electrodes and parallel to the magnetic field lines.[6] Since the electrodes protrude from the burner walls, boundary layer effects are reduced.

Although commercial magnetic flowmeters use an alternating field in order to separate the flowmeter potential from chemical polarization potentials, a permanent magnet was chosen for the magnetic flowmeter burner. A permanent magnet is well suited for the measurement of an alternating velocity field because any polarization effects (which are low frequency) can be filtered out. The use of a permanent magnet also reduces the complexity of the burner by eliminating the additional circuitry required to produce an alternating magnetic field. An ALNICO 5 permanent magnet was used in the experiments and created a magnetic field with a gap density of approximately 2100 G. The burner was constructed from 304 stainless steel, which permits the magnetic field to pass through with very little distortion.

The sonic nozzle orifice was modulated by a small-toothed gear mounted on a permanent magnet dc motor. The motor speed was controlled by a Variac adjustable autotransformer on an ac power line. The ac output of the autotransformer was converted by a rectifier bridge to a dc voltage to operate the motor. This arrangement permitted steady performance at frequencies ranging from 2000 to 20,000 Hz.

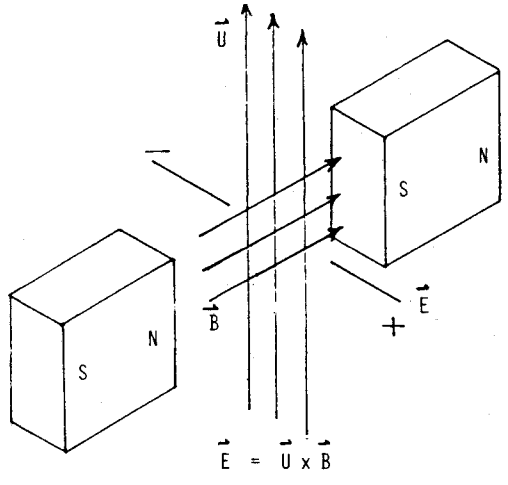

Fig. 1 Principle of operation of a magnetic flowmeter. Induced electric field is proportional to both flow velocity and magnetic field strength.

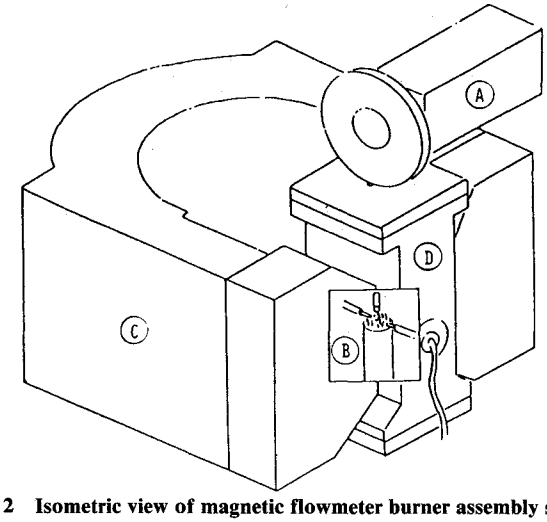

Fig. 2 Isometric view of magnetic flowmeter burner assembly showing propellant burning past pressure and velocity measurement station.

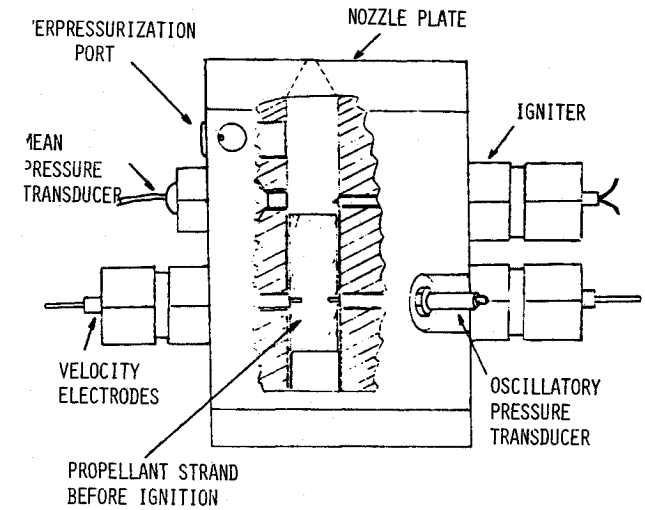

Fig. 3 Cutaway drawing of magnetic flowmeter burner showing propellant strand positioned between velocity electrodes prior to ignition.

Figure 4 presents a flowchart of the data acquisition system utilized for the magnetic flowmeter burner. The oscillatory pressure signal P' was measured by a PCB model 105A13 pressure transducer. A high pass active filter was used to remove all signal noise below 1000 Hz. The signal was then split for recording and used as a reference signal by the vector voltmeter lock-in amplifier. The lock-in amplifier, Ithaco model 393, received the velocity signal directly from the magnetic flowmeter electrodes and isolated the velocity component oscillating at the same frequency as the reference pressure signal. The output of the lock-in amplifier was the magnitude of the velocity oscillation in phase and out of phase with the pressure oscillation. These two measurements generated the real and imaginary parts of the propellant admittance function. The magnitude of P' was measured by using the rms output of a Keithley model 177 digital voltmeter. The mean chamber pressure $\bar{P}$ was measured by a Kulite model HEM-375-2000 strain-gage pressure transducer. The four data channels—the velocity oscillation magnitude in phase and 90 deg out of phase with the pressure oscillation, the magnitude of $\bar{P}'$, and the mean chamber pressure $\bar{P}$—were

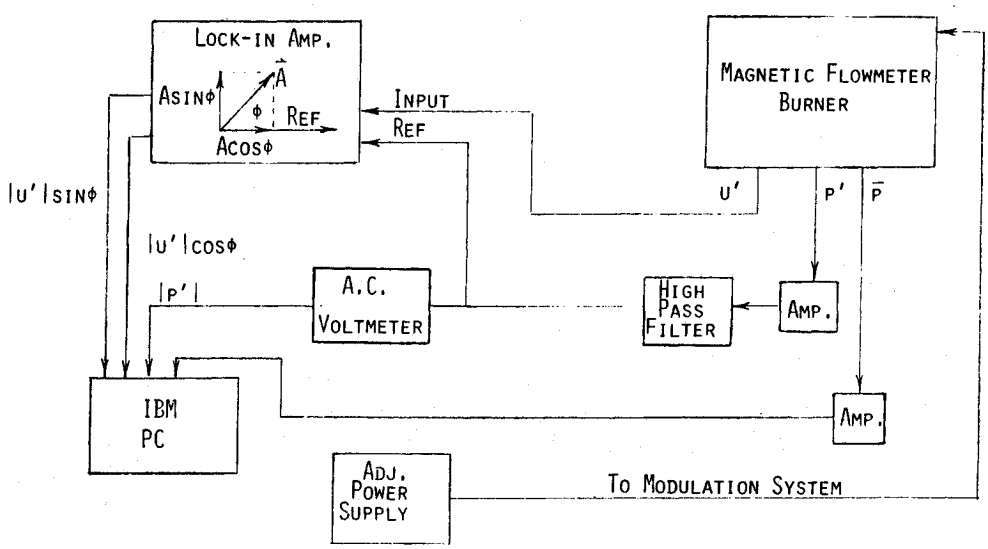

Fig. 4 Data acquisition flowchart.

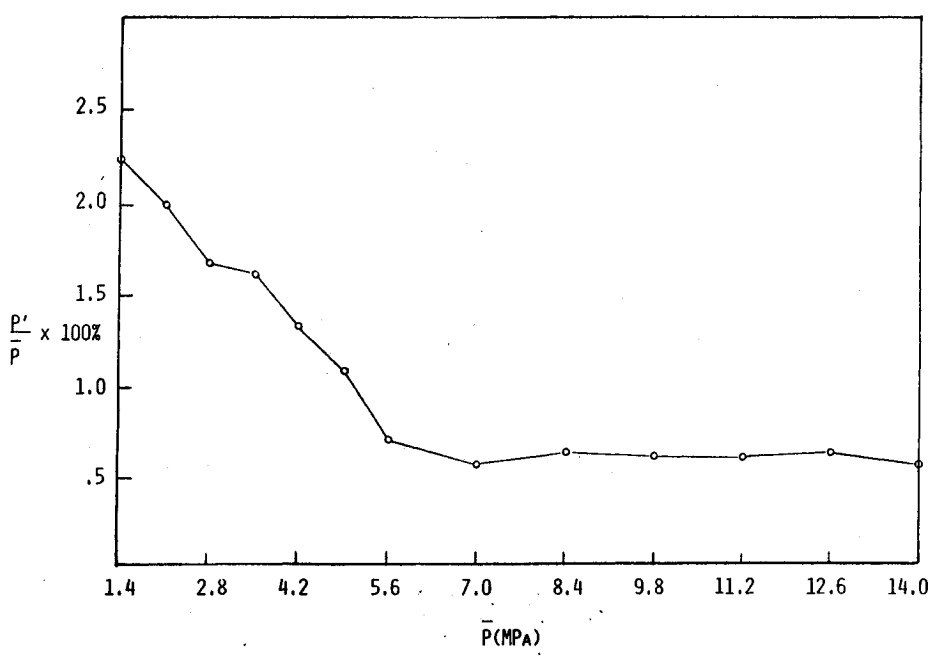

Fig. 5 Pressure oscillation amplitude vs mean chamber pressure at an excitation frequency of 20 kHz.

digitized at a sampling rate of either 20 or 250 Hz and stored on an IBM PC. Note that the oscillatory velocity and pressure were not sampled directly, but instead the lock-in amplifier and rms meter were used to preprocess the data and only the resultant magnitudes were digitized and recorded. This obviated the need for extremely high sampling rates to accurately record the high frequency signals. The moment of passage of the burning propellant surface through the measurement station is obtained by monitoring the velocity signal which is zero while the electrodes are embedded in the solid propellant.

A cold flow simulator was constructed in order to evaluate the magnetic flowmeter burner design in terms of the magnitude of pressure oscillation and the acoustic characteristics of the combustion chamber. Also, cold flow simulation was necessary to determine the effect of RTV rubber diaphragms on the transducer frequency response. The simulator duplicated the interior dimensions of the burner, with nitrogen gas forced through a porous metal plug to simulate flow from the burning propellant surface at pressure levels up to 14.0 MPa. The same motor and gear pressure modulation system to be used on the burner was applied in the cold flow simulation to determine whether it could produce pressure oscillations of sufficient amplitudes at frequencies up to 20 kHz. The theoretical acoustic characteristics were determined by approximating the chamber as a close ended cylinder. Although the cold flow simulator had mass injection at one end and outflow through the other, the closed ended cylinder approximation was used to estimate the harmonic frequencies of the various acoustic modes to guide the cold flow experiments.

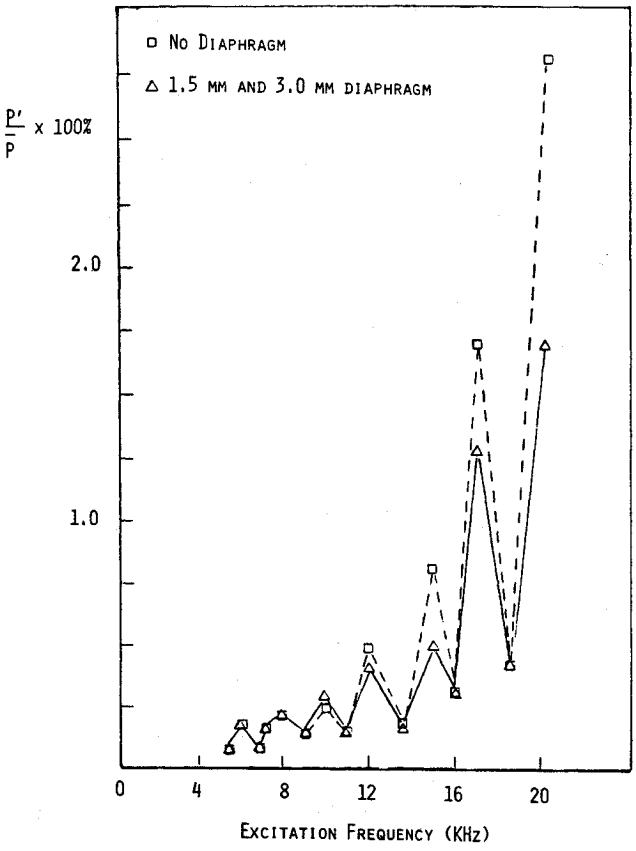

Fig. 6 Pressure oscillation amplitude vs excitation frequency for two diaphragm thicknesses at a mean chamber pressure of 3.4 MPa.

The performance of the pressure modulation system during cold flow simulation is presented in Fig. 5. The pressure oscillation amplitudes produced in the cold flow simulator are plotted as a percentage of mean chamber pressure $\bar{P}$ at an excitation frequency of 20 kHz. The oscillatory to mean pressure ratio declined initially as the mean chamber pressure rose from 1.38 to 6.9 MPa. The pressure ratio remained essentially constant from 6.9 to 13.8 MPa at a value of approximately 0.7%. The nonlinear behavior observed here is due to the complex interaction between the rotating toothed gear and the sonic nozzle orifice. The amplitude of the pressure oscillation was dependent on the mean chamber pressure and the gap between the nozzle exit plane and the teeth of the rotating gear. The gap distance that produced the largest value of P'/P was found to be approximately 3.0 mm. A slight increase in this distance resulted in a large reduction in the oscillation amplitude due to a decrease in the exit area modulation.

The cold flow simulator was also used to test the effectiveness of RTV rubber diaphragms of different thicknesses. These diaphagms were necessary to protect the pressure transducer during the combustion of the propellant. Two identical pressure transducers were mounted at the same axial location opposite each other in the cold flow simulator; one transducer had an RTV rubber diaphragm and the other was unprotected. The results of these tests are plotted in Fig. 6. The diaphragm thicknesses were 1.5 and 3.0 mm and were compared to an unprotected transducer over the frequency range of 4,000–20,000 Hz. The mean chamber pressure was held constant at 3.4 MPa. The diaphragms caused an amplitude loss that was dependent on the excitation frequency, but the phase angle between the protected and the unprotected transducers re-

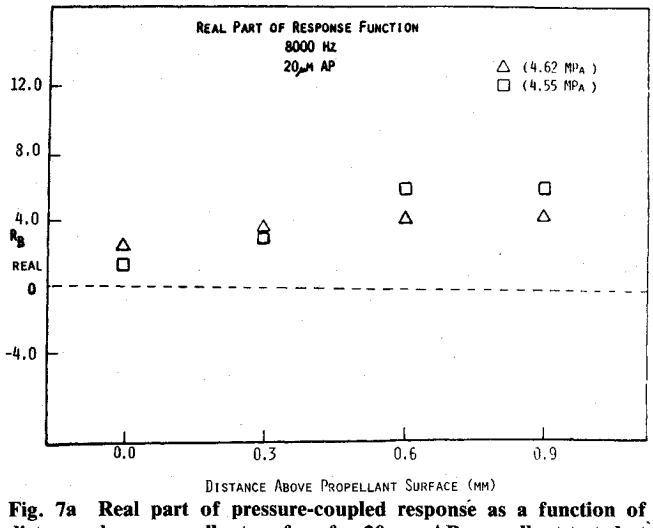

Fig. 7a Real part of pressure-coupled response as a function of distance above propellant surface for 20-μm AP propellant tested at 8000 Hz.

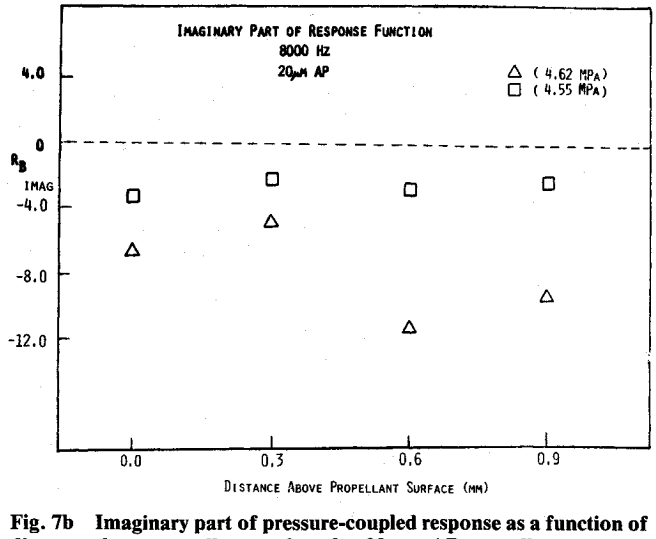

Fig. 7b Imaginary part of pressure-coupled response as a function of distance above propellant surface for 20-μm AP propellant tested at 8000 Hz.

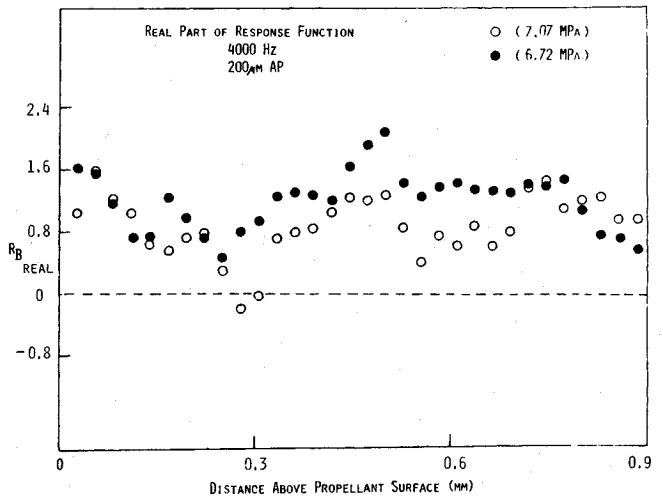

Fig. 8a Real part of pressure-coupled response as a function of distance above propellant surface for 200-μm propellant tested at 4000 Hz.

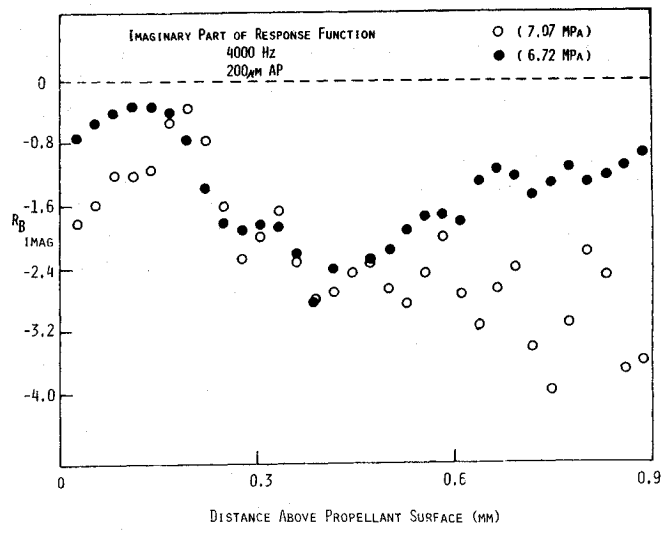

Fig. 8b Imaginary part of pressure-coupled response as a function of distance above propellant surface for 200-μm propellant tested at 4000 Hz.

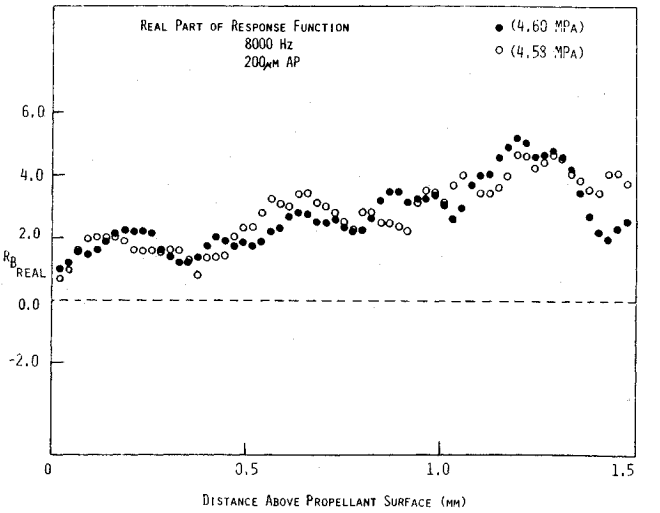

Fig. 9a Real part of pressure-coupled response as a function of distance above propellant surface for 200-μm AP propellant tested at 8000 Hz.

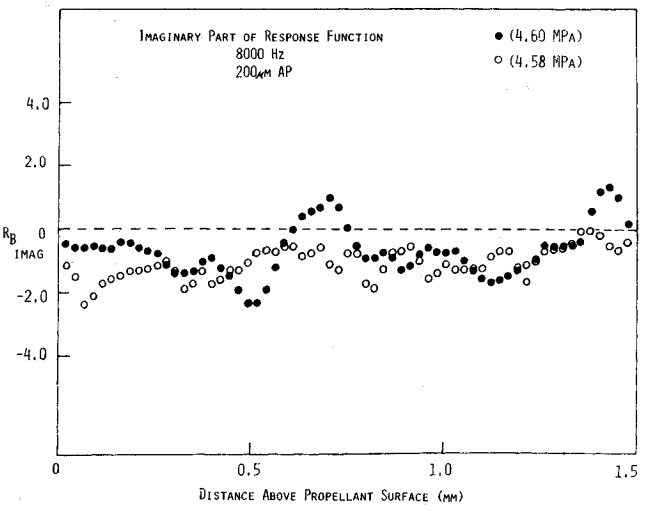

Fig. 9b Imaginary part of pressure-coupled response as a function of distance above propellant surface for 200-μm AP propellant tested at 8000 Hz.

mained zero. Although a phase angle difference between the protected and unprotected transducers was anticipated, no phase angle difference was measured over repeated tests. One possible explanation for this behavior is that the resonant frequencies of the RTV rubber diaphragms were much higher than the highest test frequency of 20 kHz. Identical results were obtained for the two thicknesses at every frequency. Based on these experimental results and design factors, the smaller diaphragm thickness was selected for use in the magnetic flowmeter burner. The amplitude loss as a function of frequency was incorporated into the data reduction. Figure 6 also displays the cold flow resonant modes. The observed amplitude peaks at frequencies less than 16,000 Hz correspond to the predicted harmonic resonant frequencies for longitudinal mode oscillation. The first observed amplitude peak occurred near the second harmonic frequency for longitudinal mode oscillations, with additional peaks occurring near each consecutive resonant frequency up to the sixth longitudinal harmonic of 15,720 Hz. Tangential mode oscillation occurred at frequencies above 16,000 Hz, creating resonant modes that were combinations of tangential and longitudinal oscillations. These combination modes were observed at two predicted resonant frequencies of 17,098 and 19,885 Hz.

The validity of the admittance measurements requires the accurate calibration of the magnetic flowmeter for both velocity signal amplitude and phase. The amplitude calibration consisted of determining the calibration constant α in Eq. (4). This was achieved by a device designed to simulate the velocity measurement in the magnetic flowmeter burner. The conducting gas flow in the burner was replaced by a solid copper rod with a diameter of 6.0 mm oriented perpendicular to both the magnetic field and the potential measuring electrodes. The electrical conductivity independence of the magnetic flowmeter equation permitted this replacement as long as the gas flow conductivity was above the limit of 10^{-3} mhos/m. An electromagnetic shaker oscillated the copper rod at frequencies up to 20 kHz in the magnetic field produced by the ALNICO 5 permanent magnet. Two graphite brushes picked up the potential across the rod, induced by the conductor moving through the magnetic field. The amplitude of the ac potential was measured by the lock-in amplifier that used a reference signal provided by the shaker power supply. The velocity of the rod was derived by integrating the acceleration measurement of a PCB model 305A05 accelerometer that had been previously factory calibrated and mounted on the top of the copper rod. The calibration data were plotted as flowmeter voltage vs oscillatory velocity of the copper rod. These data

were very consistent over a wide range of velocity amplitudes and frequencies. The ratio between velocity and voltage was inserted into Eq. (4) along with the measured magnetic field strength B and the electrode separation L yielding a calibration constant of 2.1.

A velocity signal phase calibration was required to correct the phase shift, with respect to time, induced by the inherent capacitance of the measuring circuit combined with the high gas resistance. The capacitance induces an appreciable phase shift in the velocity signal if the resistance of the combustion gas products is large. In order to quantitatively determine the phase shift that occurred in the course of the experiments, the combustion gas resistance had to be measured. Direct measurement of the gas resistance using an ohmmeter created polarization of the electrodes; therefore, an indirect method was employed to determine the gas resistance. In this indirect method, the resistance was experimentally determined by measuring the phase shift induced on an oscillatory voltage passed through the combustion gas products. The advantages of this arrangement are that it utilizes the same equipment configuration as the magnetic flowmeter burner and does not require replacing or altering the existing combustion chamber. Excellent run-to-run agreement was achieved for the gas resistance measurements obtained with the composite propellant tested at several frequencies of oscillation; the mean value of gas resistance was 40,000 Ω. The value for the gas resistance produced a maximum phase shift in the velocity measurement of 35.6 deg at a measurement frequency of 20,000 Hz, decreasing to a value of 16.0 deg at a measurement frequency of 8,000 Hz.

Admittance Measurement Results

All propellant tested was of 80% AP and 20% HTPB composition. The initial admittance data were obtained for a 20-μm unimodel AP particle size at a modulation frequency of 8000 Hz. Figures 7a and 7b plot the real and imaginary parts, respectively, of the pressure-coupled response, obtained from the measured admittance and Eq. (3), as a function of distance above the burning propellant surface. The mean sonic velocity $\bar{a}$ in Eq. (1) was calculated assuming a flame temperature of 2830 K, a ratio of specific heats γ equal to 1.17, and a molecular weight of 25.1, since no thermochemistry data were available for these propellants. The mean Mach number of the combustion product gas leaving the propellant surface was calculated using the propellant solid density ρ_s, the propellant mean gas density $\bar{\rho}_g$, the mean propellant regression rate $\bar{r}$, and the mean sonic velocity $\bar{a}$ using the equation

$$M_b = \rho_s \bar{r} / \bar{\rho}_g \bar{a} \tag{5}$$

Isentropic fluctuations are assumed, although this may not be valid near the propellant surface. The maximum distance plotted encompasses the flame zone, and the sampling rate was 20 Hz. Mean pressures for the tests ranged from 4.5 to 8 MPa and are listed for each test on Figs. 7-9. At the test pressures shown in Figs. 7a and 7b, the propellant burn rate was 0.58 cm/s. The real part of the response in Fig. 7a displays excellent reproducibility between the two runs, although the imaginary part shown in Fig. 7b does not show as good an agreement between the two runs. The sampling rate was increased to 250 Hz in order to obtain better spatial resolution for the subsequent testing of a 200-μm AP particle size propellant. Figures 8a and 8b show the real and imaginary parts, respectively, of the pressure-coupled response at a modulation frequency of 4000 Hz. The real part remains fairly constant at a value of approximately 1.0 while the imaginary part displays a change in value through the flame zone. This change starts at a value of approximately -1.0 at the propellant surface and decreases to a value of -2.5 at a distance of 0.4 mm above the propellant surface before the results of the two runs diverge at higher distances above the propellant. The propellant burn rate was 0.67 cm/s. Figures 9a and 9b show the real and imaginary parts, respectively, at a nozzle modulation frequency of 8000 Hz. At this frequency, the real part of the response increases with distance above the propellant surface, starting at a value of 1.0 at the propellant surface and rising to a value of 5.0 at a height of 1.2 mm above the surface. The imaginary part remains constant at a value of -1.0. The propellant burn rate was 0.58 cm/s.

These measured values of the pressure-coupled response are of the same order of magnitude as responses measured for similar nonmetalized composite propellants in other devices such as the T-burner. In order to obtain a value of the pressure-coupled response for use in solid rocket motor stability prediction analyses, a height above the propellant surface at which the response is defined must be chosen. Typically, the response is defined at the outer edge of the flame zone, which for composite propellants is of the order of 0.1 mm above the propellant surface. Therefore, using this assumption, the values of the pressure-coupled response at a height of 0.1 mm above the propellant surface would be the values utilized in a solid-rocket-motor stability prediction. However, the ability to measure the admittance (and therefore the response) as a function of height above the burning propellant surface can provide useful information on the effect of distributed combustion further away from the propellant surface than the normally defined flame zone thickness on the acoustic admittance.

These results can be compared with the combustion models of T'ien[7] and Flandro,[8] which incorporate unsteady gas phase reaction kinetics. Both these models calculate the oscillatory gas velocity normal to the propellant surface as a function of height above the burning propellant surface. It is this oscillatory gas velocity that constitutes the admittance defined in Eq. (1), and both models indicate that the normal oscillatory gas velocity varies in both amplitude and phase as a function of height above the propellant surface. Both models also predict that the behavior of the oscillatory normal gas velocity as a function of height above the propellant surface is strongly affected by the frequency of the forcing pressure oscillation. Thus, the experimental data obtained in this program qualitatively support the results of the unsteady gas phase models.

Conclusions

The objective of this study was to develop an apparatus that utilizes a magnetic flowmeter to obtain direct measurements of the pressure-coupled admittance for solid propellants. The magnetic flowmeter burner satisfied this objective by directly measuring the oscillatory gas velocity normal to a burning propellant surface as a function of height above the propellant surface at selected frequencies of the forcing pressure oscillations. Repeatable measurements were made for two composite propellant formulations. The magnetic flowmeter burner proved capable of measuring pressure-coupled admittances at frequencies higher than those obtainable in most other admittance or response measuring devices, and the small amount of propellant consumed by the magnetic flowmeter burner for each test makes the technique very economical for extensive testing of various solid propellants. Comparison of the experimental results with unsteady gas-phase combustion models yielded qualitative agreement.

Acknowledgments

This work was sponsored by the Air Force Rocket Propulsion Laboratory under Contract F04611-82-K-0063.

References

[1]Brown, R. S., Culick, F. E. C., and Zinn, B. T., "Experimental Methods for Combustion Admittance Measurements," *Progress in*

Astronautics and Aeronautics: Experimental Diagnostics in Combustion of Solids, edited by T. L. Boggs and B. T. Zinn, Vol. 63, AIAA, New York, 1978, pp. 191–220.

[2]Levine, J. N. and Andrepont, W. C., "Measurement Methods of Transient Combustion Response Characteristics of Solid Propellant—An Assessment," AIAA Paper 79-1209, June 1979.

[3]Semat, H., *Fundamentals of Physics*, 4th ed., Holt, Rinehart and Winston, Inc., New York, 1966.

[4]Micci, M. M. and Caveny, L. H., "MHD Measurement of Acoustic Velocities in Rocket Motor Chambers," *AIAA Journal*, Vol. 20, April 1982, pp. 516–521.

[5]Micci, M. M., "Solid Propellant Response Functions Deduced by Means of Forced Longitudinal Waves in Rocket Motors," Ph.D. Thesis, Dept. of Mechanical and Aerospace Engineering, Princeton University, Princeton, NJ, 1981.

[6]Shercliff, J. A., *The Theory of Electromagnetic Flow-Measurement*, Cambridge University Press, London, England, 1962.

[7]T'ien, J. S., "Oscillatory Burning of Solid Propellants including Gas Phase Time Lag," *Combustion Science and Technology*, Vol. 5, 1972, pp. 47–54.

[8]Flandro, G. A., "Nonlinear Transient Combustion of a Solid Rocket Propellant," AIAA Paper 83-1269, June 1983.